BIOCHEMISTRY
including biophysical chemistry & molecular biology
Article

Biochemistry **2009,** *48,* 7383–7391 7383
DOI: 10.1021/bi900631u

Characterization of an RNA-Cleaving Deoxyribozyme with Optimal Activity at pH 5[†]

Srinivas A. Kandadai,[‡] Wendy W. K. Mok,[‡] Md. Monsur Ali,[‡] and Yingfu Li*

Department of Biochemistry and Biomedical Sciences and Department of Chemistry, McMaster University, 1200 Main Street West, Hamilton, Canada L8N 3Z5. [‡]These authors have made equal contributions to this work.

Received April 13, 2009; Revised Manuscript Received July 3, 2009

ABSTRACT: An *in vitro* selection endeavor previously executed by our laboratory led to the isolation of a set of RNA-cleaving deoxyribozymes that thrive under acidic conditions [Liu, Z., Mei, S. H., Brennan, J. D., and Li, Y. (2003) *J. Am. Chem. Soc. 125*, 7539−7545]. One of these sequences, coined pH5DZ1, is a 100-nucleotide (nt) *cis*-acting enzyme that was found to exhibit high cleavage activity near pH 5. Herein, we seek to deduce the properties and sequence requirements of this enzyme. This deoxyribozyme was found to cleave a 23-nt chimeric DNA−RNA substrate, which contains a single ribonucleotide flanked by fluorophore- and quencher-modified nucleotides on each side of the cleavage junction. Extensive nucleotide deletion experiments indicated that only 42 bases within the original enzyme sequence are required for catalysis. Results from a reselection experiment further revealed that 26 of these nucleotides are absolutely conserved. In addition to sequence analysis and minimization studies, we successfully designed a *trans*-acting variant of this enzyme. Characterization of the cleavage products produced upon pH5DZ1-mediated RNA cleavage and analyses of possible structures of pH5DZ1 provided us with insights into the catalytic mechanism of pH5DZ1 and characteristics of deoxyribozymes that retain their activity under acidic conditions.

Chromosomal DNA has long been associated with the storage and transfer of genetic information. Advances in oligonucleotide synthesis and the development of *in vitro* evolution and selection strategies in recent years have led to the discovery of synthetic single-stranded sequences that are capable of catalysis (known as deoxyribozymes, DNAzymes, or catalytic DNAs) and molecular recognition (known as DNA aptamers). Presently, a collection of deoxyribozymes have been created to catalyze a diverse array of reactions (*1*). These reactions include RNA/DNA cleavage (*2*), ligation (*3*), autophosphorylation (*4*), porphyrin metalation (*5*, *6*), thymine dimer repair (*7*), carbon−carbon bond formation (*8*), and nucleopeptide linkage formation (*9*). The nature of DNA polymers renders deoxyribozymes more resistant to hydrolytic cleavage compared with naturally occurring ribozymes (*10*). *In vitro* selection can also tailor catalytic DNA sequences that remain active under a broad range of experimental conditions, including nonphysiological ones (*10*). Moreover, these synthetic DNA-based enzymes have been suggested to possess catalytic rates, efficiencies, and functional plasticity that are analogous to those of their RNA and protein counterparts (*8*, *11*, *12*).

While the isolation of deoxyribozymes with novel catalytic capabilities remains exciting in this field, current research efforts have also been diverted to characterizing existing sequences and converting them into biochemical tools and therapeutic agents (*10*, *12*). RNA-cleaving deoxyribozymes have been used to detect site-specific RNA modifications (*13*). Deoxyribozymes with catalytic activities that are dependent on specific metal ions, such as Pb^{2+} (*14*, *15*), Hg^{2+} (*16*), and Cu^{2+} (*17*), can be incorporated into sensors for such ions. Deoxyribozymes can also be covalently linked with aptamers, which are single-stranded DNA or RNA sequences capable of binding diverse targets with high affinity and specificity, in order to generate biosensors that can detect targeted molecules of interest. Known as aptazymes, these aptamer−deoxyribozyme constructs can communicate ligand binding because a change in the aptamer binding state would alter the activity of the associated deoxyribozyme (*18*, *19*). Modification of existing RNA-cleaving deoxyribozymes, such as 10-23, further gave rise to a collection of sequences with therapeutic potential (*10*, *20*). Thus far, deoxyribozymes that can specifically cleave transcripts associated with infections and many human diseases, including antibiotic resistance genes (*21*), structural genes of HIV (*22*, *23*), and oncogenes (*24*, *25*), have been engineered. A number of these deoxyribozyme-based therapeutics have entered phase I clinical trials (*10*). In addition to *in vitro* and *in vivo* applications, *in silico* applications of deoxyribozymes have also emerged in the form of deoxyribozyme-based logic gates (*26*). As the number of catalytic DNA-based tools grows, the demand for deoxyribozyme sequences whose activities will persist under a range of physiological and nonphysiological conditions is also on the rise.

Previously, our laboratory has isolated a set of deoxyribozymes that can catalyze the cleavage of a chimeric DNA−RNA substrate under acidic conditions ranging from pH 3 to pH 6 (*27*). In this substrate, the nucleotides flanking the single ribonucleotide at the cleavage junction are modified with a fluorophore on one side and a quencher on the other. Upon substrate cleavage at the appropriate pH, the fluorophore is liberated from the quencher, subsequently producing a fluorescent signal. Among the deoxyribozymes that were isolated by our group was a sequence that demonstrated the most robust activity near

[†]This work was supported by a research grant from the Natural Sciences and Engineering Research Council of Canada (NSERC). Y.L. is a Canada Research Chair. W.W.K.M. is an NSERC CGS Scholarship recipient.

*To whom correspondence should be addressed. E-mail: liying@mcmaster.ca. Tel: (905) 525-9140. Fax: (905) 522-9033.

Published on Web 07/07/2009

pH 5, with a k_{obs} of ~0.72 min^{-1}. This sequence was coined pH5DZ1.[1] In this follow-up study, we carried out a comprehensive analysis of the sequence requirements of pH5DZ1 in an effort to elucidate the nucleotides that are critical for its function and to minimize the size of the catalytic sequence. The information gathered from these analyses enabled us to design a *trans*-acting (bimolecular) variant of pH5DZ1. The minimized *trans*-acting derivative of pH5DZ1 engineered in this study can potentially reduce the cost of synthesis and be used to examine the catalytic core of this deoxyribozyme. Moreover, we examined the cleavage products of this enzyme and probed into the possible Watson−Crick helices forming its secondary structure. Collectively, these studies shed light on its mechanism of RNA cleavage and on the catalytic properties of this acidophilic enzyme.

MATERIALS AND METHODS

Oligonucleotides and Other Materials. All standard and modified DNA oligonucleotides were chemically synthesized by standard phosphoramidite chemistry (W. M. Keck Oligonucleotide Synthesis Facility, Yale University, New Haven, CT; Integrated DNA Technologies (IDT), Coralville, IA). The triisopropylsilyloxymethyl (TOM) group of the RNA linkage was removed using a previously reported method (*28*). The oligonucleotides were purified by 10% denaturing PAGE (8 M urea) prior to usage. For reselection, the partially randomized DNA library was synthesized using the following mixture of the four standard phosphoramidites (produced by manual mixing): 76% of the wild-type nucleotide and 8% of each of the remaining nucleotides. This was done following previously described protocols (*29*, *30*). Radioactive nucleotides ([γ-^{32}P]ATP and [α-^{32}P]GTP) were purchased from Perkin-Elmer (Waltham, MA). T4 DNA ligase, T4 polynucleotide kinase (PNK), calf intestine alkaline phosphatase (CIAP), and deoxyribonucleoside 5′-triphosphates (dNTPs) were purchased from MBI Fermentas (Burlington, Ontario, Canada). 2′,3′-Cyclic phosphodiesterase (CNPase) was supplied by Abnova Corp. (Taipei City, Taiwan). DNA ligation, phosphorylation, and dephosphorylation were done following manufacturer protocols using the corresponding reaction buffers. All other chemical reagents were purchased from Sigma Aldrich (Oakville, Ontario, Canada) and were used without further purification.

Catalytic assays and reselection experiments were performed in a reaction buffer containing 250 mM NaCl, 25 mM $MnCl_2$, and 50 mM sodium citrate (pH 4.8). This buffer was initially prepared as a 2× stock solution. Reactions were quenched using a 2× stop solution (80 mM EDTA (pH 8.0, 25 °C), 16 M urea, 180 mM Tris, 180 mM boric acid, 20% sucrose (w/v), 0.05% xylene cyanol, and 0.05% bromophenol blue). The antisense inhibition assay was carried out in a buffer containing 250 mM NaCl, 25 mM $MnCl_2$, and 50 mM MES (pH 6.5).

[1]Abbreviations: pH5DZ1, an RNA-cleaving deoxyribozyme with optimal function at pH 5; nt, nucleotide; k_{obs}, observed reaction rate; TOM, triisopropylsilyloxymethyl; PAGE, polyacrylamide gel electrophoresis; dNTP, deoxyribonucleoside 5′-triphosphate; PNK, T4 polynucleotide kinase; CIAP, calf intestine alkaline phosphatase; CNPase, 2′,3′-cyclic phosphodiesterase; EDTA, ethylenediaminetetraacetic acid; DTT, dithiothreitol; ssDNA, single-stranded DNA; ETA, the name for a *trans*-acting enzyme; PCR, polymerase chain reaction; ET42, the optimized *trans*-acting enzyme with 42 nucleotides; DMS, dimethyl sulfate; P5′, 5′ cleavage product.

pH5DZ1 Activity Assays. (*A*) *Assessing Activity of the Cis Constructs*. The *cis*-acting variants of pH5DZ1 were prepared by ligating the 23-nt substrate, S1, to the deoxyribozyme sequence prior to cleavage reactions following a previously established protocol (*30*). The ligated constructs were purified by 10% denaturing PAGE. The purified *cis*-acting enzyme−substrate construct was subsequently dissolved in ddH_2O so that the final concentration is 1 μM. One microliter of this construct was diluted to 0.4 μM with ddH_2O (final volume of 2.5 μL) and heated at 90 °C for 30 s. The DNA was then cooled to room temperature over 10 min. The cleavage reaction was initiated by adding 2.5 μL of the 2× reaction buffer. The reaction was conducted at room temperature for 30 min and quenched by adding 5 μL of 2× stop buffer.

(*B*) *Assessing Activity of the Trans Constructs*. The ligation step was omitted in assays performed using *trans*-acting pH5DZ1 variants. In this case, 1 pmol of the substrate was mixed with 10 pmol of the deoxyribozyme in 2.5 μL of ddH_2O. The mixture was heated at 90 °C for 30 s (to denature the DNA) and subsequently cooled to room temperature over 10 min. The cleavage reaction was initiated by adding 2.5 μL of the 2× reaction buffer. The reaction was executed at room temperature over 30 min before being quenched by the addition of the 2× stop buffer.

(*C*) *Analysis of the Cleavage Products*. The cleavage products (both *cis*- and *trans*-acting) were resolved by 10% denaturing PAGE. The gels were scanned using a Typhoon 9200 fluorimager (GE Healthcare, Baie d'Urfe, PQ, Canada), and the product bands were quantified using the ImageQuant software (Molecular Dynamics). Cleavage activity was calculated by applying the equation:

$$\% \text{ cleavage} = 100[(F_{product}/6)/[F_{substrate} + (F_{product}/6)]] \quad (1)$$

in which 6 serves as a correction factor for the difference between the fluorescence intensity of the product and that of the quencher-containing substrate (*29*). Activity assays that were done to determine the pH and metal ion dependence of pH5DZ1 were conducted following similar protocols.

Deletion Walk Experiment. The cleavage assays for the truncated *trans*-acting pH5DZ1 derivatives ETA.1 to ETA.21 were carried out using the same experimental approach described above for assessing the activities of pH5DZ1 *trans*-acting constructs. The cleavage reactions were quenched 30 min after the reaction initiation. The cleavage products were subsequently analyzed using the Typhoon 9200 scanner and the ImageQuant software as described above. The cleavage activity corresponding to each pH5DZ1 variant was calculated using eq 1. Using these data, we estimated the reaction rates (k_{obs}) associated with each pH5DZ1 mutant following background subtraction.

Antisense Inhibition Assays. *Trans*-acting pH5DZ1 (3.7 μM) and ET42 (3.7 μM) were incubated with their complementary (antisense) sequences (7.4 μM) in the presence of the aforementioned pH 6.5 buffer at 90 °C for 30 s in order to denature the DNA molecules. After cooling the samples to room temperature over 10 min, thus allowing the enzyme and antisense strands to anneal, substrate S1 (0.35 μM) and the pH 4.5 reaction buffer were added. Mixing the pH 6.5 and pH 4.5 buffers resulted in a final pH of 4.8. Negative controls were treated in a similar manner; however, antisense sequences were not added to these controls. Cleavage reactions were allowed to progress over 30 min before they were stopped by the addition of the 2× stop

buffer. The cleavage products were resolved by 10% denaturing PAGE and were visualized using the Typhoon 9200 fluorimager and analyzed by the ImageQuant software.

Characterization of Cleavage Products by Enzymatic Digestion. We followed the previously reported protocol to characterize the cleavage products by ET42 except that this experiment was done with the *trans*-acting deoxyribozyme (*29*, *31*). Substrate S3 (1 μM) was cleaved in the presence of ET42 (15 μM) in a 60 μL reaction volume over 30 min following the aforementioned assay conditions. The cleavage products were isolated by ethanol precipitation, and the resulting pellet was washed three times with 70% ethanol. The pellet was resuspended in 24 μL of ddH_2O. One microliter of this DNA mixture was subjected to each of the following enzymatic treatments: PNK, CIAP, CNPase, CNPase and PNK, and CNPase and CIAP. Reactions involving PNK and CIAP were carried out at 37 °C for 1 h in a 10 μL reaction mixture. Ten units of each enzyme was used, and the reactions were conducted in buffers supplied by the manufacturer. CNPase-mediated reactions were performed at 37 °C for 1 h in 6 μL reaction mixtures in a reaction buffer composed of 50 mM Tris-HCl (pH 7.5, 25 °C), 50 mM NaCl, 1 mM DTT, and 10% glycerol. In each of these reactions, ~5 units of CNPase was used. In reactions involving CNPase and PNK or CIAP, manufacturer supplied PNK or CIAP buffers were added to the CNPase reaction mixtures followed by the corresponding enzymes. The final volumes of these reaction mixtures were 10 μL. These reactions were conducted at 37 °C for 1 h. The reactions were subsequently stopped by heating the reaction mixtures at 90 °C for 2 min. The products were then resolved by 10% denaturing PAGE and were visualized using the Typhoon 9200 scanner and analyzed using ImageQuant.

RESULTS

Sequence and Properties of pH5DZ1. pH5DZ1 was initially isolated from a library of 100-nt single-stranded (ss) DNA sequences (with 70 central random nucleotides) through *in vitro* selection. These ssDNA molecules were ligated to a chimeric DNA−RNA substrate before being subjected to selection. Thus, the 123-nt *cis*-acting deoxyribozyme can be subdivided into two domains: a 23-nt substrate domain and a 100-nt enzyme domain (Figure 1A). Here, the nucleotides pertaining to the substrate are numbered from −1 to −23 in the 3′ to 5′ direction, while those belonging to the deoxyribozyme are numbered from +1 to +100 in the 5′ to 3′ direction. In the deoxyribozyme sequence, the first 15 nucleotides at each end of the enzyme constitute the "binding arms" for PCR primers, which allow the sequences to be amplified following each round of selection. Removal of the nucleotides in these regions did not interfere with the activity of pH5DZ1. 5′ and 3′ deletion studies further revealed that the first 24 nucleotides in the 5′ end and the last 17 nucleotides in the 3′ end were dispensable for the function of this deoxyribozyme.

As it was mentioned above, this substrate contains a single adenosine ribonucleotide at the cleavage site. This ribonucleotide (denoted "R") is located at position −9 of the sequence, and it is flanked by a fluorophore (F; a fluorescein-modified thymine deoxyribonucleotide) on its 5′ side and a quencher (Q; a DABCYL-modified thymine deoxyribonucleotide) on its 3′ side. Although the cleavage reaction was previously observed to occur optimally at a pH of 4.8, pH5DZ1 exhibits activity between pH 4.0 and pH 5.5 (Supporting Information Figure S1). This reaction is also dependent on the presence of divalent metal ions

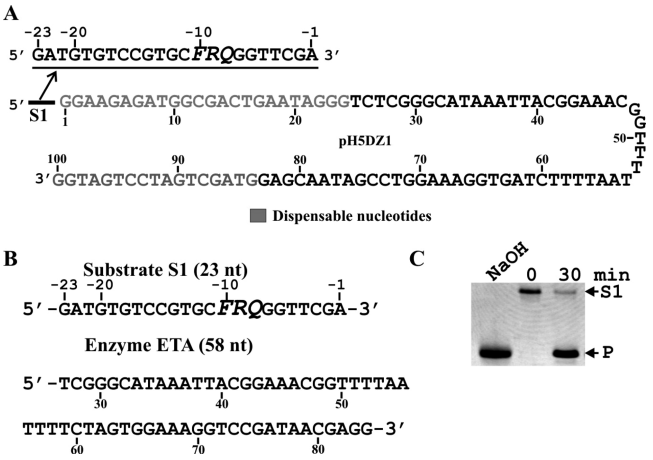

FIGURE 1: Sequence and activity of pH5DZ1 and its truncated derivative ETA. (A) The primary sequence of pH5DZ1. The original *cis*-acting deoxyribozyme sequence is divided into two modules: the chimeric substrate (S1) and the catalyst. Nucleotides in the substrate are numbered as −1 to −23 in the 3′ to 5′ direction. In the catalyst region, nucleotides are numbered from +1 to +100 in the 5′ to 3′ direction. The ribonucleotide at the cleavage junction within S1 and its flanking fluorophore- and quencher-modified residues are italicized. The first 24 nucleotides and the last 17 nucleotides within the catalyst sequence were found to be dispensable. These nucleotides, which are highlighted in gray, include the 5′ and 3′ primer-binding arms. (B) Removal of the dispensable nucleotides from the 5′ and 3′ ends resulted in the production of a *trans*-acting variant of pH5DZ1, which was named ETA (*trans*-acting enzyme A). The nucleotides in ETA are numbered according to their positions in the full-length pH5DZ1. (C) Cleavage activity of ETA was evaluated under single-turnover conditions by reacting 0.2 μM S1 with 2.0 μM of ETA following a 30 min reaction. F = fluorescein-dT, Q = DABCYL-dT, and R = adenine ribonucleotide.

(Supporting Information Figure S2). We compared the cleavage yield of pH5DZ1 in the presence of various divalent metal ions while keeping all other experimental conditions constant. Under these conditions, we observed that the deoxyribozyme generated the highest quantity of cleavage product in the presence of Mn^{2+}, indicating that Mn^{2+} is preferred over other ions. This preference for Mn^{2+} is a characteristic common to many RNA-cleaving deoxyribozymes (*32*).

Design of the Trans-Acting Deoxyribozyme. Nearly all of the *cis*-acting RNA-cleaving deoxyribozymes that have been isolated to date have been successfully converted into *trans*-acting catalytic sequences. This collection of *trans*-acting deoxyribozymes not only includes sequences that function at neutral pH but it also encompasses a few of the acidic pH-dependent sequences that were reported by our laboratory. In contrast to *cis*-acting sequences, these *trans*-acting deoxyribozymes are less expensive and are more facile to use, since it is not necessary to ligate substrates to these enzymes prior to cleavage reactions. Here, we sought to derive a *trans*-acting variant of pH5DZ1.

The engineering of a *trans*-acting deoxyribozyme requires the substrate and enzyme modules to be separated into two molecules. The observation that the first 24 nucleotides of pH5DZ1 can be removed from the *cis*-acting construct without interfering with its activity suggests that the two modules may be divided at the substrate−catalyst junction. The *trans*-acting system designed in this way was found to be active indeed. We further found that the length of the *trans* catalyst could be reduced to 58 nt by removing 26 nt and 17 nt from the 5′ and the 3′ termini, respectively. This resulting sequence, referred to as ETA (*trans*-acting enzyme; Figure 1B), remains fully active. When the

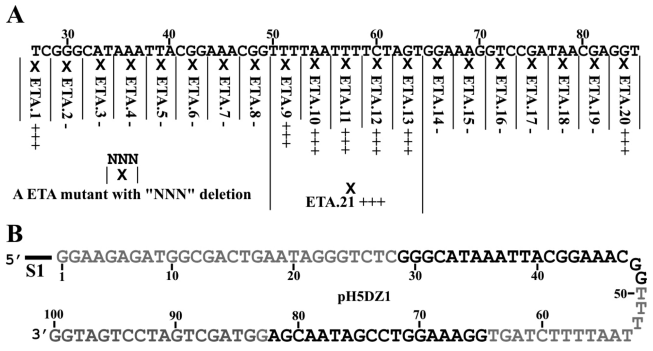

FIGURE 2: Deletion mutants of ETA. (A) The sequences of ETA and its deletion mutants with the truncated nucleotides indicated. Deletion mutants ETA.1−20 were produced by removing three nucleotides from the sequence at a time, whereas mutant ETA.21 was generated by the removal of the 15 nucleotides between T_{50} to T_{64}. The cleavage activity of each construct is scored by (+) and (−) symbols. (−) denotes no activity, (+) denotes $k_{obs} < 1.0 \times 10^{-4}$ min^{-1}, (++) denotes $k_{obs} = (1.0-9.9) \times 10^{-4}$ min^{-1}, (+++) denotes $k_{obs} = (1.0-9.9) \times 10^{-3}$ min^{-1}, and (++++) denotes $k_{obs} = (1.0-9.9) \times 10^{-2}$ min^{-1}. (B) Results from the "deletion walk" experiments. The activity of each mutant construct indicates that nucleotides 1−28, 50−64, and 83−100 are not obligatory for catalysis.

cleavage reaction was carried out under single turnover conditions with 1 μM S1 and 10 μM ETA, over 30% of the substrate was cleaved following 30 min of reaction time (Figure 1C).

Minimizing the Sequence of ETA. Our initial sequence minimization efforts suggested that the functionally important residues of pH5DZ1 reside between nucleotides 25 and 83. In addition to introducing deletions to the 5′ and 3′ ends of pH5DZ1, we produced a series of deletion mutants by sequentially deleting 3 nt of the sequence starting at T_{25} in order to further minimize the size of the deoxyribozyme (Figure 2). We assessed the reaction yield of each of these mutants at 30 min after the reaction initiation (data not shown). For simplicity, we assigned a score for the activity of each mutant based on a system that was previously used by our group (*30*): sequences given a score of (++++) are considered to be efficient catalysts with an estimated k_{obs} of ≥0.01 min^{-1} (≥10% cleavage in 10 min), sequences assigned a score of (+++) have an estimated k_{obs} between 0.01 and 0.001 min^{-1} (≥10% cleavage in 100 min), a score of (++) correspond to a k_{obs} between 0.001 and 0.0001 min^{-1} (≥10% cleavage in 1000 min), while sequences with a score of (+) are considered to be poor catalysts with a k_{obs} of 0.00001 min^{-1} or less (< 10% cleavage in 1000 min). Sequences assigned a score of (−) are considered inactive, since cleavage was not detected within 1000 min of reaction time. Results from this "deletion walk" experiment indicate that the nucleotides between T_{50} and T_{64} are entirely dispensable, since their removal did not appear to have an impact on the cleavage activity of pH5DZ1, as demonstrated by sequences ETA.9 through ETA.13. Likewise, nucleotides T_{27} and C_{28} (sequence ETA.1) along with the last three nucleotides from the 3′ end of ETA (sequence ETA.20) can be deleted without altering the function of the enzyme. Deleting the other nucleotides in the sequence was found to be deleterious to the activity of the deoxyribozyme. Collectively, these results indicate that an additional 20 nt can be removed from pH5DZ1 without reducing its catalytic efficiency.

Probing for Catalytically Important Residues by Reselection. Our deletion walk efforts provided us with insights into the sequence requirement of pH5DZ1, but we still sought to examine the significance of individual nucleotides within the conserved region of the deoxyribozyme. After we removed the dispensable bases from the 5′ and 3′ ends of the enzyme, 59 nucleotides remained. The length of this sequence renders it challenging to generate mutations at each base via single-nucleotide mutation strategies (such as site-directed mutagenesis) since a large number of sequences will first have to be systematically produced before their functions can be examined. Consequently, we turned to DNA library synthesis and reselection to circumvent this problem. We implemented a selection strategy that was similar to the one used in the isolation of the parent pH5DZ1 sequence (*27*). The library used for reselection consisted of sequences that were 89 nt in length, as they lack the nonessential nucleotides residing in the 5′ and 3′ ends of pH5DZ1. Every nucleotide in the 59-nt enzyme sequence was mutagenized at a rate of 24%, such that they had a 76% chance of being the wild-type nucleotide and an 8% chance of being each of the other three nucleotides. The sequence corresponding to the enzyme was flanked by primer-binding arms on each end. For reselection with this partially randomized DNA library, we designed a new set of primers which were different from the ones used in the original *in vitro* selection experiment in order to prevent cross-contamination by the wild-type deoxyribozyme.

Since the *in vitro* selection experiment has been extensively described in previous studies, we will only provide a brief synopsis here (*30*). The enzyme, substrate, template, and primer sequences used in reselection are illustrated in Figure 3A. The selection scheme is outlined in Figure 3B. Prior to the first round of selection, the library of pH5DZ1 derivatives (denoted L1) was ligated to the substrate sequence (S2) in the presence of a template sequence (T1) and T4 DNA ligase. These 106-nt constructs were purified by 10% denaturing PAGE prior to being subjected to cleavage reactions in the presence of the selection buffer. Following cleavage, the 91-nt 3′ cleavage fragments were once again purified by denaturing PAGE. These fragments were subsequently subjected to two rounds of PCR. The first round of amplification was performed using primers P1 and P2. The 5′ primer, P1, introduces a 5′ overhang to the enzyme following amplification. These 106-bp products were amplified using primers P2 and P3. PCR amplification using P3 introduces a ribonucleotide to the leading strand before the start of L1, thereby allowing the single-stranded L1 to be regenerated following alkaline digestion and separation from the lagging strand. The single-stranded L1 molecules were ligated to S2 following 5′ phosphorylation by PNK, allowing a new round of selection to be initiated.

While a low percentage of the molecules (2−10%) exhibited self-cleavage in the first four rounds of reselection (Figure 3C), higher cleavage activity was detected by the fifth round (G5) in which ~20% of self-cleavage activity was detected. Although a higher cleavage activity was observed in G6, we cloned and sequenced 39 clones from G5 rather than G6 in order to avoid repeatedly isolating the dominant species. Sequencing results and the variations observed at each position of the mutant sequences are summarized in Supporting Information Figure S3. Results from the reselection experiment indicated that 23 nucleotides within the pH5DZ1 sequence are absolutely conserved (as depicted in green in Figure 3D). These nucleotides are mainly located in two regions, one between A_{35} and C_{47} and the other between T_{72} and A_{78}. Nine nucleotides within the sequence are considered highly conserved (highlighted in blue in Figure 3D). These bases include C_{28}, G_{29}, A_{33}, C_{41}, G_{63}, G_{65}, G_{66}, A_{69}, and A_{80}. The results further revealed that 26 nucleotides in the

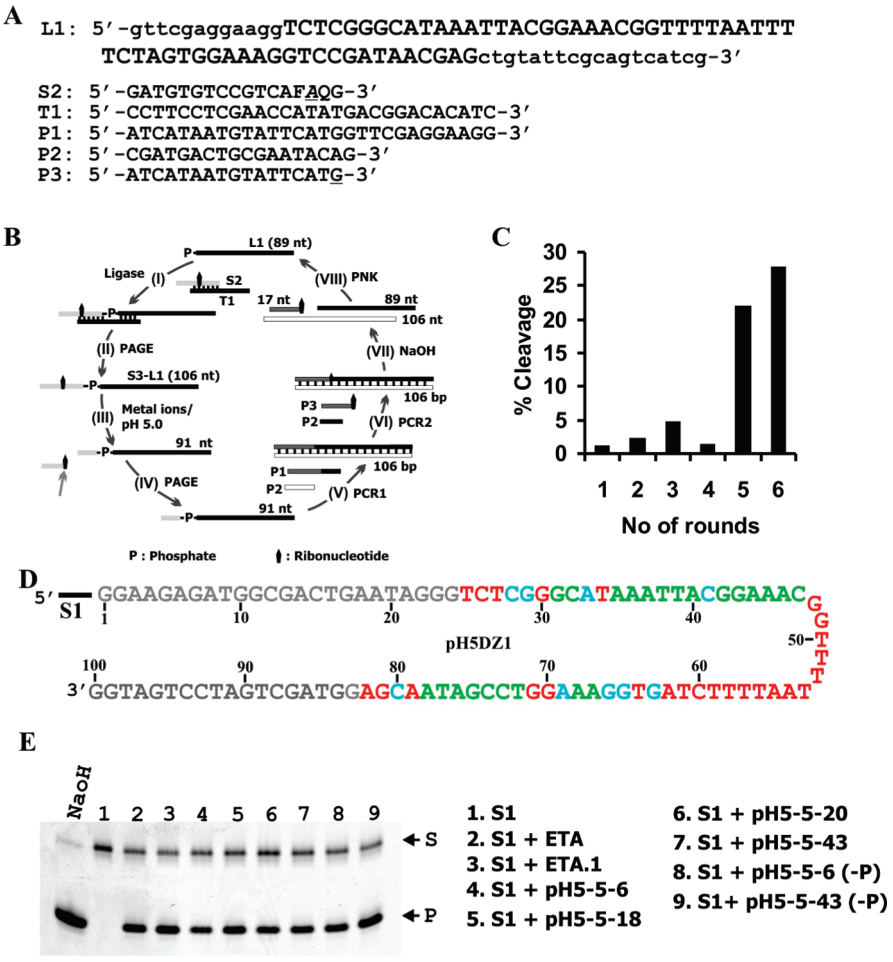

FIGURE 3: Reselection of active pH5DZ1 mutants. (A) DNA sequences used for *in vitro* selection. The lower-case letters in L1 signify primer-binding sites. The other letters of the sequence denote nucleotides that were partially randomized in order to generate the library used for selection. In S2, the italicized "R" represents the adenosine ribonucleotide at the cleavage junction. The underlined "G" in P3 denotes the guanine ribonucleotide at the end of the primer. (B) Selection scheme. Each selection cycle consists of eight steps, numbered I−VIII here. (I) The 89-nt catalytic sequence (L1) is ligated to substrate S2. (II) The 106-nt S2−L1 ligation product is purified by PAGE. (III) The ligation product is subjected to cleavage reaction in the presence of divalent metal ions at pH 5.0. (IV) The 91-nt 3′ cleavage fragment is isolated by PAGE and is amplified using primers P1 and P2 (V). (VI) The 106-nt PCR product is amplified again using P2 and P3 in order to introduce a ribonucleotide in L1. (VII) The dsDNA is treated with NaOH to cleave the leader sequence at the ribonucleotide. (VIII) This cleavage fragment is phosphorylated at the 5′ end and is subjected to a second round of selection. (C) Progress of reselection. (D) Sequence analysis of mutants isolated after G5. Comparing mutations observed in each of the 39 active sequences obtained following this round of selection provided information pertaining to the conservation of nucleotides at each position of pH5DZ1. Letters in red represent variable nucleotides, letters in blue are indicative of important residues, and letters in green symbolize essential and absolutely conserved bases. Sequences of the pH5DZ1 derivatives isolated at G5 are presented in Figure S3. (E) Fluorescent image of the cleavage activity of four deoxyribozyme sequences isolated from G5. The substrate in the leftmost lane was cleaved by NaOH as opposed to pH5DZ1 or its derivatives. In lanes 8 and 9, substrates were cleaved by derivatives of pH5-5-6 and pH5-5-43, which were chemically synthesized without primer-binding arms (as indicated by "−P" beside their names).

sequence can be changed without hindering catalysis, including nucleotides between G_{48} and A_{62} (noted in red in Figure 3D). This observation coincides with the finding from the "deletion walk" experiment, in which it was found that nucleotides within this region can be completely removed without affecting the catalytic activity of pH5DZ1 (Figure 2B).

To ascertain that the reselected pH5DZ1 mutants are catalytically active, we selected four clones, pH5-5-6, pH5-5-18, pH5-5-20, and pH5-5-43, and subjected them to a cleavage assay (Figure 3E). Two of these sequences, pH5-5-6 and pH5-5-43, were chemically synthesized without the two primer-binding arms, as denoted by "−P" beside their names in Figure 3E. All sequences were incubated with substrate S1 for 30 min prior to being analyzed by PAGE. The substrates and products were visualized by fluorimaging (Figure 3E). The activities of these mutant sequences were observed to be comparable to the activity of the minimized wild-type sequence, ETA. Removal of primer-binding arms did not appear to affect the activity of these pH5DZ1 derivatives. Combining the data from the deletion walk experiment and that from the reselection experiment, we further reduced the size of the deoxyribozyme to 42 nt by removing nucleotides from 50 to 64, which were shown to be dispensable. This optimized sequence was named ET42, and its sequence is presented in Figure 5A.

Deducing the Secondary Structure of pH5DZ1 by Covariations. In an effort to deduce the secondary structure of pH5DZ1, we obtained putative secondary structures by computational means, using the mfold secondary structure prediction program (*33*), and by visual inspection based on our previous experience. These efforts generated three possible structures with minimized *trans*-acting sequence. These include a structure with a three-way junction (Figure 4A), one with a triple helix (triplex, Figure 4B), and one with a three-stem motif (Figure 4C). The Watson−Crick base-pairing interactions that may have taken

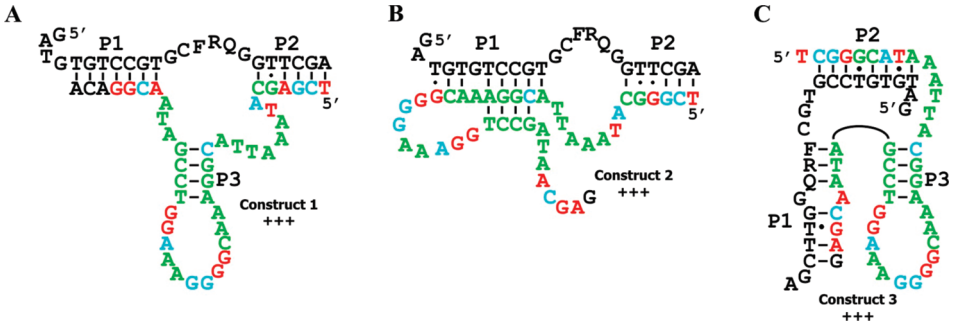

FIGURE 4: Predicted secondary structures of minimized pH5DZ1 derivatives. The three putative structures were obtained using the mfold secondary structure prediction program (*33*) and by visual inspection. These include (A) the three-way junction, (B) the triple helix (triplex), and (C) the three-stem structures. These three clones were chosen from our reselection experiment (Supporting Information Figure S3). The color scheme is identical to Figure 3.

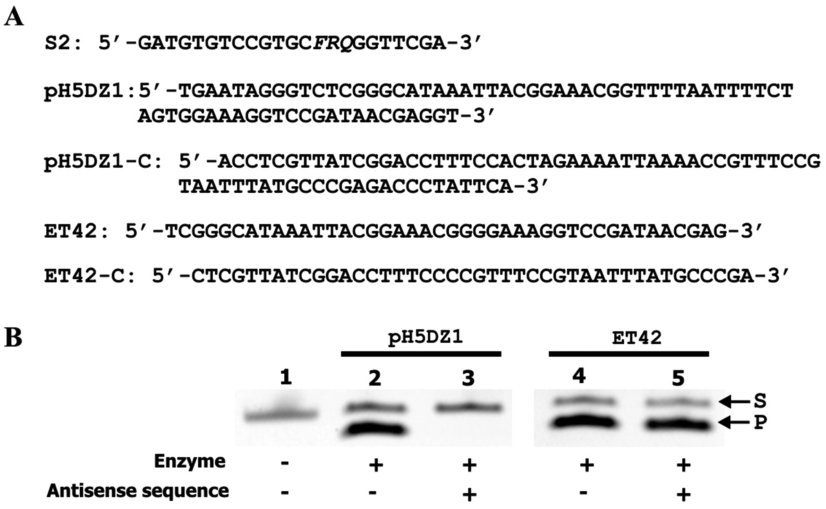

FIGURE 5: Inhibition of pH5DZ1 and ET42-mediated RNA cleavage using complementary sequences. (A) Sequences of substrate (S2), pH5DZ1, ET42, and their respective complementary counterparts (pH5DZ1-C and ET42-C). (B) Effects of complementary (antisense) sequences on catalysis. pH5DZ1 and ET42 in lanes 3 and 5 were allowed to anneal to their respective antisense sequences in the presence of a pH 6.5 buffer prior to the addition of the chimeric substrate and a pH 4.5 reaction buffer, which adjusted the reaction pH to 4.8. In lanes 2 and 4, the deoxyribozymes were not treated with their antisense sequences before catalysis. The cleavage reaction was allowed to occur in the presence of divalent metal ions at pH 4.8 over 30 min. The substrate was added alone in lane 1 and served as control. Cleavage products were resolved by 10% denaturing PAGE and visualized using a fluorimager.

place to give rise to each of the predicted conformations were tested by covariation studies. We observed that in all of these constructs mutations introduced into each potential stem of the sequence obliterated its catalytic activity. For example, in the three-way junction structure, point mutations introduced into stem P1 hindered the substrate cleavage, even when those mutations preserved the integrity of the stem, as seen in the first two structures in the left panel (Supporting Information Figure S4A). Likewise, substitutions introduced to stem P2 resulted in a loss of catalytic activity (structures in the right panel). These included a substitution that strengthened the base pairing in the stem by replacing a G-T wobble with a T-A base pair (the second structure in the right panel). While some of these mutations may have removed nucleotides that are involved in folding of the deoxyribozyme into its tertiary structure or in catalysis, the lack of experimental data supporting any of the putative secondary structures insinuates that the catalytic structure of this deoxyribozyme may be formed solely based on non-Watson−Crick interactions, which is a possibility at an acidic pH of 4.8 (see Discussion).

Antisense Inhibition of pH5DZ1 and ET42. To examine whether Watson−Crick base pairing occurs at pH 4.8 and gives rise to the active structure, we carried out an antisense inhibition assay. In this assay, pH5DZ1 and ET42 were incubated with their respective complementary (antisense) sequences in the presence of a pH 6.5 buffer prior to the addition of the substrate and the pH 4.5 reaction buffer (Figure 5A). Hybridization between the deoxyribozymes and their antisense counterparts was anticipated to sequester the deoxyribozymes, consequently preventing substrate binding and cleavage when the pH reached 4.8 following the addition of the pH 4.5 buffer. After pH5DZ1 was incubated with its antisense sequence, its catalytic activity was abolished, suggesting that the enzyme was bound by its complementary sequence (Figure 5B, left panel). On the other hand, the activity of ET42 was not affected by the presence of its antisense sequence (Figure 5B, right panel). At pH 6.5, Watson−Crick base pairing is likely to be the predominant mode by which the two strands interact. However, at a lower pH, this form of base pairing is likely to be interrupted and replaced by other forms of base pairing, such as hemiprotonated $C \cdot C^+$ interactions (*34*). This can cause the helix to be less stable, favoring the dissociation of the two strands. pH5DZ1, which is 28 nt longer than ET42, was expected to form a stronger interaction with its antisense sequence than ET42 (*34*). As such, when the pH was lowered

following hybridization of the enzyme and its antisense strand, the DNAzyme was less likely to fully dissociate from its complementary strand to adopt its catalytically active structure.

At this time, we are unable to provide a conclusive structure of this deoxyribozyme based on our mutagenesis data. Data from dimethyl sulfate (DMS) methylation interference assays performed with the ET42 sequence did not offer much information concerning catalytically important residues or the catalytic structure, though it implicated three guanine residues in catalysis or in folding into the active structure, since methylation at the N7 position of these residues interfered with cleavage activity (Supporting Information Figure S5). These nucleotides corresponded to the conserved guanines G_{16}, G_{17}, and G_{34}. As mentioned above, the cleavage activity observed after ET42 was exposed to its antisense sequence implies that its catalytically active conformation may be dominated by non-Watson−Crick interactions. Further experiments are required to elucidate the secondary structure of this deoxyribozyme and precisely pinpoint the nucleotides that are involved in substrate cleavage.

Characterization of pH5DZ1 Cleavage Products. The phosphoester-transfer mechanism of RNA cleavage catalyzed by pH5DZ1 was examined following a previously published protocol (*28*, *30*). This mechanism is of particular interest to us, because at an acidic pH of 4.8, the deprotonation of the 2′-hydroxyl nucleophile is expected to be more difficult. As such, the cleavage mechanism of pH5DZ1 may differ from that of a deoxyribozyme that functions at neutral pH. In this study, the cleavage products were subjected to enzymatic digestions in order for the 5′ cleavage product to be traced by fluorimaging. Substrate cleavage by the deoxyribozyme can produce either a 5′ cleavage product (P5′) with a 2′- or 3′-monophosphate terminus or one with a 2′,3′-cyclic phosphate terminus. To deduce which of the three products was synthesized, the substrate was incubated with ET42 for 30 min, and the product mixture was then treated with various phosphodiesterases. These enzymes included T4 polynucleotide kinase (PNK), which has 2′,3′-cyclic nucleotide 3′-phosphodiesterase activity in addition to 2′- and 3′-phosphatase activity, calf intestine alkaline phosphatase (CIAP), which has 2′- and 3′-phosphatase activity but not 2′,3′-cyclic phosphodiesterase activity, and 2′,3′-cyclic nucleotide 3′-phosphodiesterase (CNPase), which can hydrolyze 2′,3′-cyclic phosphate to 2′-phosphate. Following enzymatic treatment, the sequences were resolved by 10% denaturing PAGE. This allows for changes in the mobility of P5′, which is associated with the terminal phosphate, to be traced.

Treating the cleavage products with PNK decreased the migration of P5′ due to the loss of negative charges associated with the phosphate group (Figure 6, lane 3). CIAP treatment, on the other hand, did not affect the migration of P5′ (Figure 6, lane 4). This suggests that P5′ contains a cyclic terminal phosphate. Likewise, CNPase treatment did not retard the movement of P5′ on the gel (Figure 6, lane 5). To further explore the nature of the product, we treated the cleavage products with CNPase followed by PNK (Figure 6, lane 6) or CIAP (Figure 6, lane 7). Both of these enzyme combinations resulted in decreased mobility of P5′ on the gel. Collectively, these analyses demonstrate that pH5DZ1- or ET42-mediated cleavage produces a 5′ cleavage fragment with a 2′,3′-cyclic phosphate and a 3′-cleavage fragment with a 5′-OH, much like the products generated following cleavage by all naturally occurring self-cleaving ribozymes and synthetic RNA-cleaving nucleic acid enzymes.

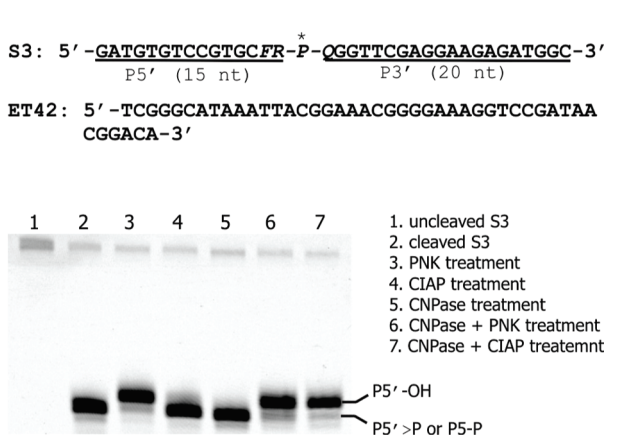

FIGURE 6: Characterization of pH5DZ1 cleavage products by enzymatic digestion. (A) Sequences of substrate S3 and the minimized *trans*-acting pH5DZ1 derivative ET42. The phosphorus atom residing in the phosphoester linkage at the cleavage junction is indicated (*P). The substrate may be divided into two parts: the 15-nt 5′ cleavage product (P5′) and the 20-nt 3′ cleavage product (P3′). (B) Determining the chemical nature of the phosphate at the 3′ end of P5′ by enzymatic digestion. In lane 1, the substrate was not subjected to deoxyribozyme cleavage. The band corresponding to the product in lane 2 was produced after treating S3 with NaOH (0.25 M) at 90 °C over 10 min. In lanes 3−5, the substrate was cleaved by ET42. The products were subsequently isolated and were treated with polynucleotide kinase (PNK, lane 3), calf intestine alkaline phosphatase (CIAP, lane 4), and 2′,3′-cyclic nucleotide 3′-phosphodiesterase (CNPase, lane 5). Cleavage products in lanes 6 and 7 were first treated with CNPase followed by PNK (lane 6) or CIAP (lane 7). Each reaction mixture was analyzed on 10% denaturing PAGE. The fluorescence signal associated with P5′ was then traced by scanning the gel using a fluorimager. P5′-OH indicates P5′ with a hydroxyl group in its 3′ terminus. P5′ > P or P5′-P indicates P5′ with a 2′,3′-cyclic phosphate or a 2′- (or 3′-) monophosphate group in its 3′ terminus.

DISCUSSION

pH5DZ1 was previously isolated from a random sequence library through an *in vitro* selection experiment conducted at pH 5 (*27*). This 100-nt *cis*-acting enzyme was found to cleave a chimeric DNA−RNA substrate, which contains a single ribonucleotide at the cleavage junction. This substrate was designed such that the ribonucleotide is flanked by a fluorophore-modified nucleotide on one side and a quencher-modified nucleotide on the other. Hence, once it is cleaved, the fluorophore is freed from the quencher and a fluorescent signal is consequently generated. Due to this modification, this deoxyribozyme offers a unique choice for biosensor engineering when appended to aptamers that can bind targets of interest. Before we can take advantage of this unique deoxyribozyme as a useful molecular tool, however, it is highly beneficial to understand its sequence, structural, and catalytic properties. For this purpose, we examined the sequence requirements for pH5DZ1-mediated RNA cleavage and investigated possible secondary structures of this deoxyribozyme with its substrate. To produce a more cost-effective and efficient deoxyribozyme, we converted pH5DZ1 into a *trans*-acting system, coined ETA (Figure 1C). We further minimized the deoxyribozyme sequence by removing redundant nucleotides from the 5′ and 3′ ends, which served as primer-binding arms in our initial selection experiment. The necessity of internal nucleotides for catalysis was analyzed by sequentially removing three nucleotides at a time and evaluating the activity of each deletion mutant (Figure 2). The conservation of each nucleotide was investigated through a reselection experiment using a library

of randomized sequences based on pH5DZ1. Sequencing results obtained from 39 sequences isolated following five rounds of reselection revealed that 23 nucleotides within the pH5DZ1 are absolutely conserved and 9 nucleotides are highly conserved (Supporting Information Figure S3). Twenty-six nucleotides were found to be hypermutated. These nucleotides coincide with those that were found to be dispensable from the deletion walk experiment. On the basis of the results gathered from these experiments, we reduced the size of pH5DZ1 from 100 nt to 42 nt, and this *trans*-acting, optimized sequence was named ET42.

After we had established a series of functional *trans*-acting sequences, we sought to deduce their possible secondary structures. Using mfold as well as by visual inspection, we proposed three possible secondary structure models. We attempted to verify these models by changing the identities of nucleotides that are involved in the predicted stems. However, we did not succeed in producing a verifiable structural model using covariation analysis. Our task of structural elucidation may be complicated by the fact that this deoxyribozyme is most active at pH 5. Under such conditions, the formation of non-Watson−Crick base pairs within the deoxyribozyme or between the enzyme and substrate may be favored. At acidic pH, the N3 position of cytosine residues is expected to be protonated. Under these circumstances, fundamental forces, such as hydrogen bonding and electrostatic interactions between these positively charged bases and the phosphodiester backbone, are anticipated to prevail. Moreover, the formation of hemiprotonated $C^+ \cdot C$-type base pairs or Hoogsteen-type $CG \cdot C^+$ triplets would also be possible.

Compared to well-characterized RNA-cleaving deoxyribozymes that function at neutral pH, such as 10-23 and 8-17, the minimized size of pH5DZ1 is nearly twice as large (*35*). The larger size was also previously observed with the minimal sequences of pH3DZ1 and pH4DZ1, RNA-cleaving enzymes with optimal activity at pH 3 and pH 4, respectively (*28*, *29*). It was speculated that the lack of effective Watson−Crick interactions resulted in the need for a large number of nucleotides in the formation of the deoxyribozyme's tertiary structure. This may also be the case for pH5DZ1.

We wish to continue to pursue the structure of pH5DZ1 using high-resolution techniques, such as X-ray crystallography and NMR, in the near future. This information would be valuable to us in engineering tools based on this enzyme. Once the residues that make up the substrate binding arms and the catalytic core are discerned, we can determine where we can append aptamers in order to produce a pH5DZ1-based aptazyme without drastically affecting the catalytic activity of the enzyme. Knowing where the substrate binding arms are or deducing the nucleotides within the deoxyribozyme that are responsible for interacting with the substrate would enable us to modify these regions in order to produce a collection of deoxyribozymes for specific biosensing applications under matching acidic conditions. Efforts in our laboratory are underway to design pH5DZ1-based biosensors.

ACKNOWLEDGMENT

We thank members of the Li laboratory for helpful discussions with regard to the project and the manuscript.

SUPPORTING INFORMATION AVAILABLE

The pH profile of pH5DZ1 (Figure S1), the metal ion dependence of pH5DZ1 (Figure S2), DNA sequences of mutants isolated from reselection experiments (Figure S3), covariation analysis data (Figure S4), and data from our dimethyl sulfate interference assay (Figure S5). This material is available free of charge via the Internet at http://pubs.acs.org.

REFERENCES

1. Silverman, S. K. (2008) Catalytic DNA (deoxyribozymes) for synthetic applications-current abilities and future prospects. *Chem. Commun.* (*Cambridge*) 3467–3485.
2. Breaker, R. R., and Joyce, G. F. (1994) A DNA enzyme that cleaves RNA. *Chem. Biol. 1*, 223–229.
3. Cuenoud, B., and Szostak, J. W. (1995) A DNA metalloenzyme with DNA ligase activity. *Nature 375*, 611–614.
4. Li, Y., and Breaker, R. R. (1999) Phosphorylating DNA with DNA. *Proc. Natl. Acad. Sci. U.S.A. 96*, 2746–2751.
5. Li, Y., and Sen, D. (1996) A catalytic DNA for porphyrin metallation. *Nat. Struct. Biol. 3*, 743–747.
6. Li, Y., Geyer, C. R., and Sen, D. (1996) Recognition of anionic porphyrins by DNA aptamers. *Biochemistry 35*, 6911–6922.
7. Chinnapen, D. J., and Sen, D. (2004) A deoxyribozyme that harnesses light to repair thymine dimers in DNA. *Proc. Natl. Acad. Sci. U.S.A. 101*, 65–69.
8. Chandra, M., and Silverman, S. K. (2008) DNA and RNA can be equally efficient catalysts for carbon-carbon bond formation. *J. Am. Chem. Soc. 130*, 2936–2937.
9. Pradeepkumar, P. I., Hobartner, C., Baum, D. A., and Silverman, S. K. (2008) DNA-catalyzed formation of nucleopeptide linkages. *Angew. Chem., Int. Ed. Engl. 47*, 1753–1757.
10. Baum, D. A., and Silverman, S. K. (2008) Deoxyribozymes: useful DNA catalysts in vitro and in vivo. *Cell. Mol. Life Sci. 65*, 2156–2174.
11. Breaker, R. R., Emilsson, G. M., Lazarev, D., Nakamura, S., Puskarz, I. J., Roth, A., and Sudarsan, N. (2003) A common speed limit for RNA-cleaving ribozymes and deoxyribozymes. *RNA 9*, 949–957.
12. Schlosser, K., and Li, Y. (2009) Biologically inspired synthetic enzymes made from DNA. *Chem. Biol. 16*, 311–322.
13. Hengesbach, M., Meusburger, M., Lyko, F., and Helm, M. (2008) Use of DNAzymes for site-specific analysis of ribonucleotide modifications. *RNA 14*, 180–187.
14. Liu, J., and Lu, Y. (2003) Improving fluorescent DNAzyme biosensors by combining inter- and intramolecular quenchers. *Anal. Chem. 75*, 6666–6672.
15. Liu, J., and Lu, Y. (2004) Accelerated color change of gold nanoparticles assembled by DNAzymes for simple and fast colorimetric Pb^{2+} detection. *J. Am. Chem. Soc. 126*, 12298–12305.
16. Lee, J. S., and Mirkin, C. (2008) Chip-based scanometric detection of mercuric ion using DNA-functionalized gold nanoparticles. *Anal. Chem. 80*, 6805–6808.
17. Liu, J., and Lu, Y. (2007) Colorimetric Cu^{2+} detection with a ligation DNAzyme and nanoparticles. *Chem. Commun.* (*Cambridge*), 4872–4874.
18. Chiuman, W., and Li, Y. (2007) Efficient signaling platforms built from a small catalytic DNA and doubly labeled fluorogenic substrates. *Nucleic Acids Res. 35*, 401–405.
19. Elbaz, J., Shlyahovsky, B., Li, D., and Willner, I. (2008) Parallel analysis of two analytes in solutions or on surfaces by using a bifunctional aptamer: applications for biosensing and logic gate operations. *ChemBioChem 9*, 232–239.
20. Dass, C. R. (2004) Deoxyribozymes: cleaving a path to clinical trials. *Trends Pharmacol. Sci. 25*, 395–397.
21. Hou, Z., Meng, J. R., Zhao, J. R., Hu, B. Q., Liu, J., Yan, X. J., Jia, M., and Luo, X. X. (2007) Inhibition of beta-lactamase-mediated oxacillin resistance in *Staphylococcus aureus* by a deoxyribozyme. *Acta Pharmacol. Sin. 28*, 1775–1782.
22. Bano, A. S., Gupta, N., Sharma, Y., Sood, V., and Banerjea, A. C. (2007) HIV-1 VprB and C RNA cleavage by potent 10−23 DNAzymes that also cause reversal of G2 cell cycle arrest mediated by Vpr genes. *Oligonucleotides. 17*, 465–472.
23. Sood, V., Unwalla, H., Gupta, N., Chakraborti, S., and Banerjea, A. C. (2007) Potent knock down of HIV-1 replication by targeting HIV-1 Tat/Rev RNA sequences synergistically with catalytic RNA and DNA. *AIDS 21*, 31–40.
24. Zhang, G., Dass, C. R., Sumithran, E., Di Girolamo, N., Sun, L. Q., and Khachigian, L. M. (2004) Effect of deoxyribozymes targeting c-Jun on solid tumor growth and angiogenesis in rodents. *J. Natl. Cancer Inst. 96*, 683–696.
25. Dass, C. R., Choong, P. F., and Khachigian, L. M. (2008) DNAzyme technology and cancer therapy: cleave and let die. *Mol. Cancer Ther. 7*, 243–251.

26. Willner, I., Shlyahovsky, B., Zayats, M., and Willner, B. (2008) DNAzymes for sensing, nanobiotechnology and logic gate applications. *Chem. Soc. Rev. 37*, 1153–1165.
27. Liu, Z., Mei, S. H., Brennan, J. D., and Li, Y. (2003) Assemblage of signaling DNA enzymes with intriguing metal-ion specificities and pH dependences. *J. Am. Chem. Soc. 125*, 7539–7545.
28. Mei, S. H., Liu, Z., Brennan, J. D., and Li, Y. (2003) An efficient RNA-cleaving DNA enzyme that synchronizes catalysis with fluorescence signaling. *J. Am. Chem. Soc. 125*, 412–420.
29. Ali, M. M., Kandadai, S. A., and Li, Y. (2007) Characterization of pH3DZ1-An RNA-cleaving deoxyribozyme with optimal activity at pH 3. *Can. J. Chem. 85*, 261–273.
30. Kandadai, S. A., and Li, Y. (2005) Characterization of a catalytically efficient acidic RNA-cleaving deoxyribozyme. *Nucleic Acids Res. 33*, 7164–7175.
31. Kandadai, S. A., Chiuman, W., and Li, Y. (2006) Phosphoester-transfer mechanism of an RNA-cleaving acidic deoxyribozyme revealed by radioactivity tracking and enzymatic digestion. *Chem. Commun.* (*Cambridge*), 2359–2361.
32. Wang, W., Billen, L. P., and Li, Y. (2002) Sequence diversity, metal specificity, and catalytic proficiency of metal-dependent phosphorylating DNA enzymes. *Chem. Biol. 9*, 507–517.
33. Zuker, M. (2003) Mfold web server for nucleic acid folding and hybridization prediction. *Nucleic Acids Res. 31*, 3406–3415.
34. Leroy, J. L., Gehring, K., Kettani, A., and Gueron, M. (1993) Acid multimers of oligodeoxycytidine strands: stoichiometry, base-pair characterization, and proton exchange properties. *Biochemistry 32*, 6019–6031.
35. Santoro, S. W., and Joyce, G. F. (1997) A general purpose RNA-cleaving DNA enzyme. *Proc. Natl. Acad. Sci. U.S.A. 94*, 4262–4266.